



ELSEVIER

journal homepage: www.elsevier.com/locate/jmatprotec

Nanocrystalline titanium produced by hydrostatic extrusion

Wacek Pachla^{a,*}, Mariusz Kulczyk^{a,b}, Malgorzata Sus-Ryszkowska^b,
Andrzej Mazur^a, Krzysztof J. Kurzydowski^b

^a Institute of High Pressure Physics, Polish Academy of Sciences (Unipress), Sokolowska 29/37, 01-142 Warszawa, Poland

^b Warsaw University of Technology, Faculty of Materials Science and Engineering, Woloska 141, 02-507 Warszawa, Poland

ARTICLE INFO

Article history:

Received 8 March 2007

Received in revised form

22 October 2007

Accepted 14 November 2007

Keywords:

Severe plastic deformation

Hydrostatic extrusion

Grain refinement

Nanocrystalline

Titanium

ABSTRACT

Commercial purity titanium (CP-Ti) grade 2 was hydrostatically extruded (HE) in 20 consecutive passes with cumulative true strain of 5.47 without intermediate annealing. HE results in a significant grain refinement. The grain size was reduced from $\sim 33 \mu\text{m}$ to nanometre scale of equivalent grain diameter 47 nm. The refinement of the structure was accompanied by enormous enhancement of the mechanical properties with the ductility retained at the level characteristic of other bulk severe plastic deformation (SPD) treated materials ($\sim 8\%$). The ultimate tensile strength, $\text{UTS} > 1300 \text{ MPa}$ and yield stress, $\text{YS} \sim 1250 \text{ MPa}$, the highest ever reported for bulk CP-Ti samples, were measured after HE. These values are higher than those of the solution treated (hardened) Ti-Al-V commercial alloy. The Hall-Petch (H-P) strength and hardness relations have shown to be not congruent. For the YS dependence the linear fit seems to be appropriate, while the hardness dependence reveals the slope change from positive (material hardening with decreasing grain size) to negative (material softening). The threshold falls at $\sim 120 \text{ nm}$, around the point commonly considered to be the UFG/NC microstructure transformation border. The results obtained revealed the possibility fabricating long-length high strength nanocrystalline CP-Ti semi-products using the hydrostatic extrusion (HE) process. Such semi-products can be used in medicine, e.g. for dental implants, where high strength and good biocompatibility are required.

© 2007 Elsevier B.V. All rights reserved.

1. Introduction

One of the necessary conditions to induce a nanocrystalline (NC) or ultra-fine grained (UFG) microstructure into solids is to generate severe plastic deformation (SPD) by a metalforming operation. Special methods of mechanical deformation must be used to generate NC structures in bulk materials. SPD of bulk forms is mostly performed by consecutively repeating single deformation passes during the processes such as rolling (called accumulative roll bonding ARB (Saito et al., 1999)), multiple (uniform) forging (Salishchev et al., 1999) or equal channel angular pressing (called ECAP (Valiev and Langdon, 2006)). All these processes, except ECAP, lead to a decrease of the dimen-

sions of the samples and changes in their geometry. With high strength materials, such as titanium or its alloys, SPD techniques are often performed at elevated temperatures where the increased ductility and reduction in the yield strength promote large-strain deformation. However, elevated temperatures should be avoided wherever possible to reduce the thermally activated recovery and recrystallization processes that result in unwanted grain growth. Only a few cold work processes have been applied for SPD of titanium.

Up till now, cold ECAP (Nagasekhar et al., 2006), cold ARB (Dinda et al., 2005), ECAP at 410°C (Woo-Jin Kim et al., 2006), ECAP between 350 and 450°C + cold rolling CR (Stolyarov et al., 2003), ECAP at 450°C + cold extrusion (Stolyarov et al., 2001a),

* Corresponding author. Tel.: +48 22 632 5010; fax: +48 22 632 4218.

E-mail address: wacek@unipress.waw.pl (W. Pachla).

0924-0136/\$ – see front matter © 2007 Elsevier B.V. All rights reserved.

doi:10.1016/j.jmatprotec.2007.11.103

Table 1 – The initial mechanical properties and chemical composition of commercially pure Ti (CP-Ti grade 2)

Ultimate tensile strength, UTS (MPa)	546
Yield stress, YS (MPa)	439
Microhardness, HV _{0.2} (MPa)	2010
Strain to fracture, ϵ_f (%)	23.6
Element (weight %)	
C	<0.01
H	<0.001
N	0.01
O	0.16
Fe	0.08
Ti	Balance

ECAP at 400 °C + cold rolling (Valiev et al., 2004), forging at 400 °C (Salishchev et al., 2006) and high pressure torsion HPT at room temperature (Valiev et al., 2002) have been utilized for pure titanium in the SPD processes.

One of the method which induces SPD in high strength materials at room temperature and quite recently has confirmed its usefulness in NC or UFG generation is cumulative hydrostatic extrusion (HE) (Pachla et al., 2006; Kurzydowski, 2006a,b). The main type of deformation in HE is elongation along the product axis while in most of the other processes it is shearing. According to Segal (2002), a simple shear in narrow bands is the most efficient for the formation of UFG structures. This paper describes the technique for producing bulk NC structures in CP-Ti after severe deformation at room temperature. The properties of commercial purity titanium after SPD with use of HE are presented and compared with the results obtained by other SPD processes.

2. Experimental procedure

Commercially pure titanium 99.74%, with the specification corresponding to ASTM B 348-GR2, annealed and smooth turned (cold) was investigated. Table 1 shows the composition of the CP-titanium. The initial structure of the CP-Ti is shown in Fig. 1.

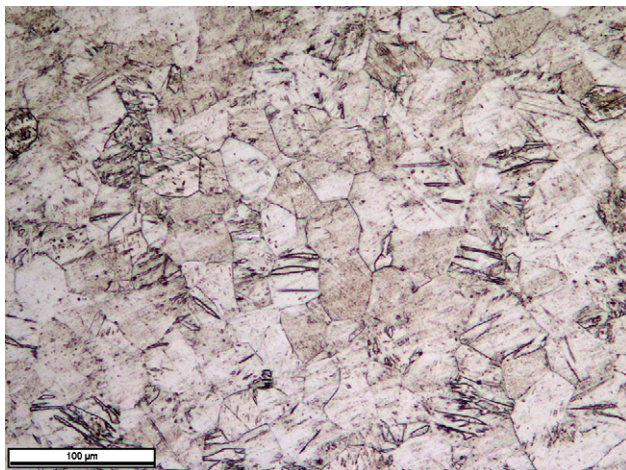


Fig. 1 – Light microscopy micrograph of the CP-Ti before starting hydrostatic extrusion (rod OD = 50 mm).

In order to quantify changes in the grain size, the equivalent diameter of grain projections, d_2 , was used (this diameter is defined as the diameter of a circle which has the surface area equal to the surface area of a given grain). The mean equivalent diameter $E(d_2)$ and the variation coefficient $CV(d_2)$ defined as the ratio of the standard deviation to the mean value, were determined in more than 100 randomly selected grains. The values of the mean equivalent grain diameter $E(d_2) \sim 33 \mu\text{m}$ and the small spread of the standard deviation of the grain sizes $S.D.(d_2) = 7.8 \mu\text{m}$ characterise the initial material from which the starting billet with OD = 50 mm (and 300 mm in length) was made. The initial mechanical properties of CP-Ti are given in Table 1. The material was hydrostatically extruded to form a round wire of 3.25 mm in diameter in 20 passes with cumulative true strain of 5.47. Extrusion was performed at two Unipress hydroextrusion presses, one of bore diameter 65 mm operating to maximum pressure 1.2 GPa, and the second of bore diameter 31 mm and 1.7 GPa maximum pressure. A $2\alpha = 45^\circ$ angle of the die and a special combination of lubricants based on PTFE and MoS₂ were used. No intermediate annealings were performed between the extrusion passes. The mean percentage reduction per pass rpp% during the first 7 passes was 36.2% and during the remaining 13 passes it was 15.6%. The extrusion strain rate gradually increased from 0.8 s^{-1} in the first pass up to $3.28 \times 10^2 \text{ s}^{-1}$ in the last one.

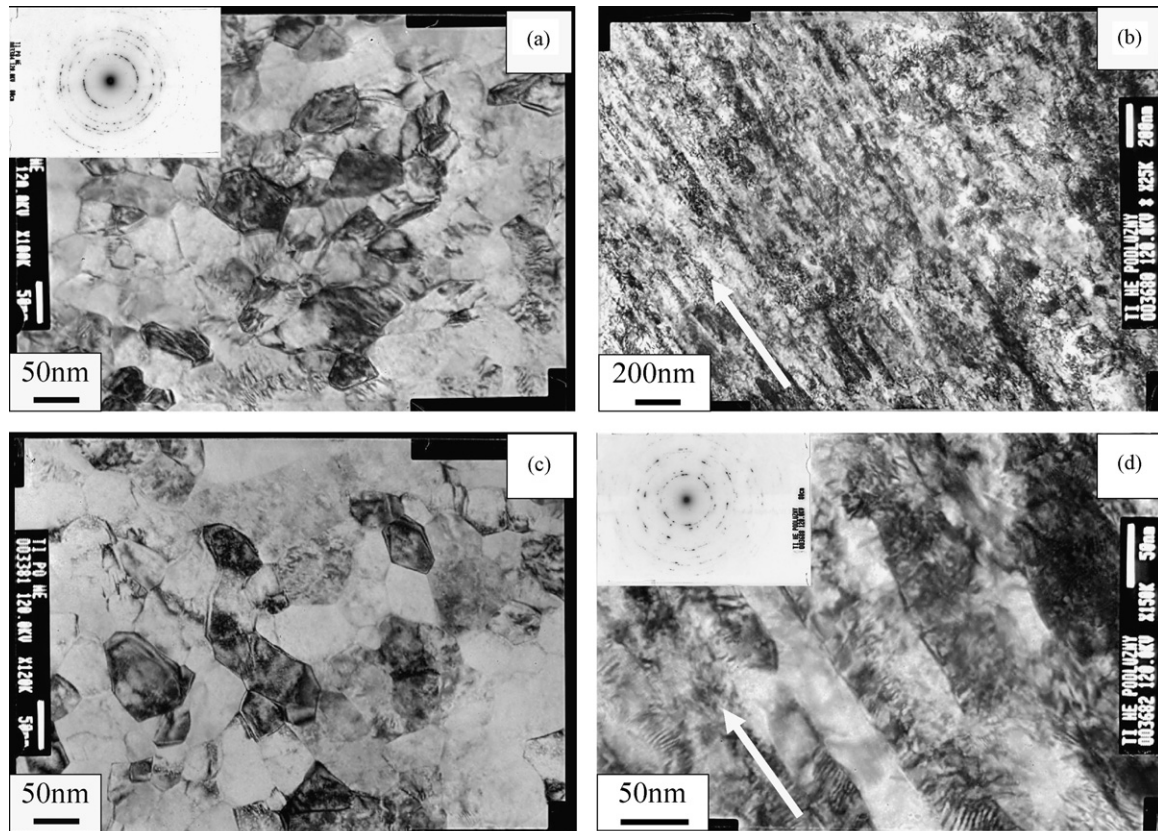
Microstructures of the processed samples were investigated by transmission electron microscopy Jeol 1200 using an acceleration voltage of 120 keV. The transverse and longitudinal cross-sections of the extruded wires were observed. The ultimate strength, yield stress and elongation to failure were measured by Unipress tensile machine (force accuracy $\pm 1\text{N}$, strain accuracy $\pm 1 \mu\text{m}$) at room temperature with a strain rate of $2 \times 10^{-3} \text{ s}^{-1}$ during tensile (length to diameter factor 5) and compression (height to diameter factor 1.5) tests of samples 3.25 mm in diameter. Vickers microhardness, HV, was measured by Zwick-Roell ZHV1-A hardness tester across the wire diameter under a load of 0.2 kg applied by 15 s.

3. Results and discussion

3.1. Microstructure

3.1.1. Transverse section

Typical TEM micrographs and the selected area diffraction (SAD) pattern from a transverse section of CP-Ti processed by hydrostatic extrusion in 20 passes are shown in Fig. 2(a and b). The SAD pattern indicates the existence of a large fraction of high-angle boundaries (circled spots), but the presence of clustered diffraction spots suggests that low-angle boundaries also exist, inset in Fig. 2(a). The observed elongation of the diffraction spots indicates the existence of elongated crystallites and residual stresses caused by the excessive elastic strains. The grain size was reduced from approximately $33 \mu\text{m}$, Fig. 1, to the nanometre scale—the mean value of the equivalent grain diameter $E(d_{eq})$ was 47 nm, i.e. was reduced more than 700 times, Fig. 2. Such a mixture of various, non-equilibrium grain boundaries (low-angle and high-angle boundaries) could be beneficial for the properties of this metal, especially the strength to ductility ratio (Valiev, 2004). The



Note: white arrows indicate direction of extrusion axis

Fig. 2 – TEM micrographs and SAD pattern from (a and b) transverse section and (c and d) longitudinal section, of CP-Ti processed by hydrostatic extrusion in 20 passes with cumulative true strain $\varphi = 5.47$.

grain size distribution was relatively homogeneous with a mono-modal histogram, Fig. 3, and the coefficient of variation $CV(d_2)$ was below 0.3. This is evidence that the processed sample microstructure is homogeneous (Kurzydowski and Ralph, 1995). The grain refinement was more than twice as efficient and much more homogeneous than that observed in

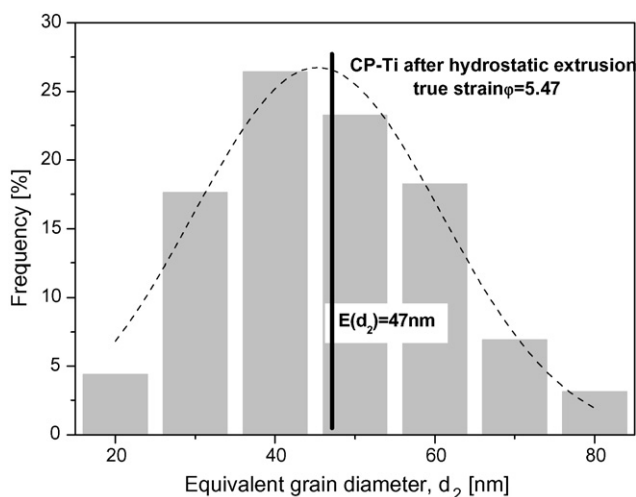


Fig. 3 – Grain size distribution in CP-Ti processed by hydrostatic extrusion in 20 passes with cumulative true strain $\varphi = 5.47$.

CP-Ti after deformation with true strain of 3.82 evaluated as $E(d_2) = 87$ nm and $CV(d_2) > 0.49$ (Pachla et al., 2006; Garbacz et al., 2006). Due to the limited number of slip planes, deformation twinning boundaries are not observed in the transverse sections. On the basis of numerous TEM observations we can infer that the grain interiors are very differentiated in quality. Some have a higher dislocation density and less sharp grain boundaries, the other are better healed with sharp grain boundaries. This can confirm that low-angle and high-angle boundaries are present in the microstructure. Especially, observations realized at the various inclinations of the TEM samples confirm this fact. The regularity of the grain shapes observed on transverse sections increases with decreasing grain size, the grains being, in general, equiaxed ones. It should be noted that the volume fraction of the grains below 45 nm is almost 50% and the smallest grains are below 20 nm.

Summarized data of the true strain dependence of the mean grain size and the yield stress after the various SPD processes applied to CP-Ti are plotted in Fig. 4. A sharp drop of grain size is observed for strains below true strain of ~ 5 when the mean grain size decreases from ~ 1000 nm size to 50–300 nm, i.e.: by 70–95%. A further increase of strain does not bring about visible grain refinement. On the contrary, the weak tendency of grain coarsening with increasing strain can be seen in Fig. 4(a). The smallest grain sizes in transverse sections were measured after the HPT, ECAP combined with thermo-mechanical-treatment TMT and HE processes within

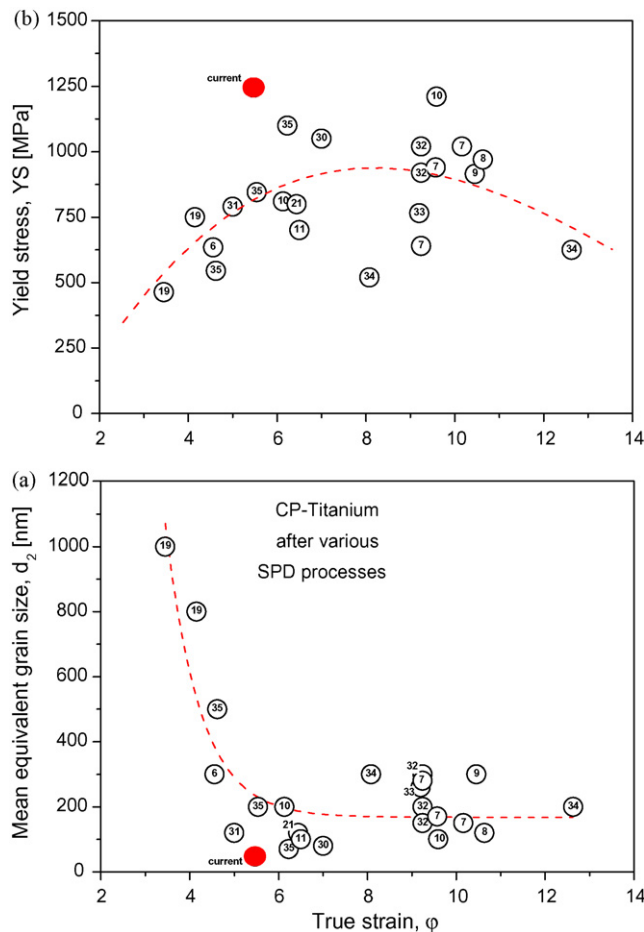


Fig. 4 – Mean equivalent grain size (a) and yield stress (b) for CP-Ti processed by various SPD processes; note: references in the circles.

the range of true strains from 5 to 7. The highest values of the yield stress were also measured within this range, Fig. 4(b).

3.1.2. Longitudinal section

Fig. 2(c and d) shows a longitudinal section of the extruded wire with cumulative strain of 5.47. In general, the longitudinal nanostructure can be characterized as oriented (inhomogeneous) fibrous with a high dislocation density. Crystallites with internal cells are also observed. It can be seen from Fig. 2(c and d) that, in the longitudinal direction, the microstructure is laminar. These crystallites exist within the localized deformation bands elongated in the extrusion direction (axis of the extruded wire). The deformation twins occur very seldom, which is rather unusual, since they should be more common in longitudinal sections, where they play a significant role in the formation of elongated grains and accommodation of the shear strains. This can be explained by the presence of localized deformation bands. The elongated bands are well textured of ~50–100 nm in width and segmented into equiaxed-like nanometric grains approximately of the same ~50 nm diameter as those observed in the transverse section, Fig. 2(a and b). High dislocation density and blurred grain boundaries are common in the longitudinal section.

This was also confirmed by TEM observations performed at various sample inclination angles. The numerous diffraction circles indicate the existence of high-angle grain boundaries, whereas the elongation of diffraction spots indicates the presence of internal stress and elongation of the grains, Fig. 2(d). The non-uniformity dislocation of the contrast within the bands and the fuzzy boundaries of the structural elements also indicate that high internal stresses have been induced (Stolyarov et al., 2001a, 2005).

The lack of twins in the final nanostructure was also observed after other SPD processes such as twist extrusion TE (Stolyarov et al., 2005) or ECAP (Stolyarov et al., 2003) above a certain accumulated true strain level. This suggests that in HE at high strains, the twinning system is replaced by the dislocation slip system which operates more efficiently.

3.2. Mechanical properties

3.2.1. Ultimate tensile strength and yield stress

Tensile stress–strain curves for the starting rod (50 mm) and the final wire (3.25 mm) are presented in Fig. 5. For comparison, the compression test result for the final wire is also shown. The value of the ultimate tensile strength increased from 546 MPa in the starting material to 1320 MPa after 20 HE passes, which corresponds to a cumulative true strain of 5.47. The corresponding increase of the yield stress was from 439 to 1245 MPa. This is an enormous improvement of the mechanical strength, over 140% increase of the ultimate tensile strength and over 180% increase of the yield stress compared to the values measured in the starting material and far above the values obtained for CP-Ti after processing by a combination of ECAP (8 passes) with cold extrusion (75% reduction) (Stolyarov et al., 2001a). The values obtained after hydrostatic extrusion are also higher, by 13% (both UTS and YS), than those of the solution treated Ti-6Al-4V alloy (ASTM Grade 5) commonly used for blades, airframes, forgings and biomedical implants. The compression yield stress was measured to be 900 MPa, Fig. 5, i.e. it is lower by 27% than the tensile yield stress. Usually but not always, compression leads to higher values than those

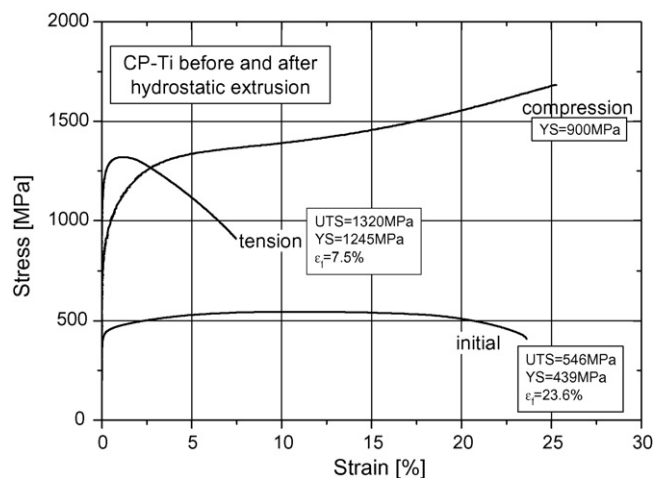


Fig. 5 – Tensile stress–strain curves for the starting CP-Ti rod (50 mm) and the final wire (3.25 mm) after hydrostatic extrusion in 20 passes with cumulative true strain $\phi = 5.47$.

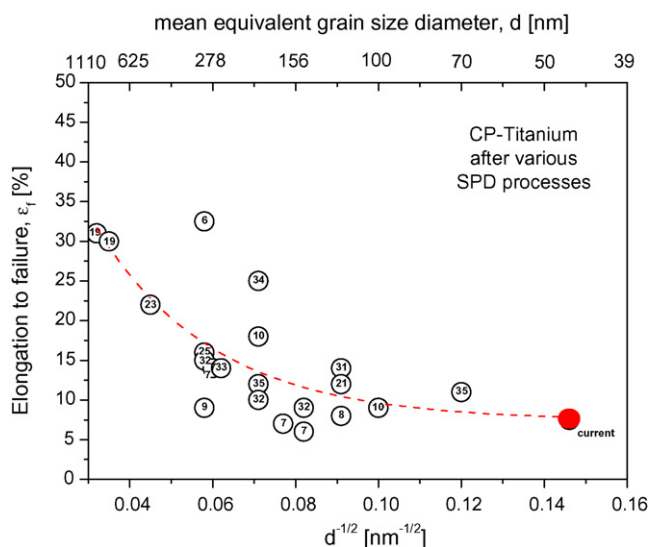


Fig. 6 – Elongation to failure as a function of the mean equivalent grain size for CP-Ti processed by various SPD processes; note: references in the circles.

measured in tensile tests (ASTM Grade 5), thus this relation is surprising and difficult to explain.

3.2.2. Elongation to fracture

A significant decrease by almost 70% in elongation to failure ε_f was observed in the final product after 20 passes of hydrostatic extrusion. Thus, the results obtained are disappointingly low. Although, the absolute value of $\varepsilon_f = 7.5\%$ is comparable to the results reported by other investigators, who however used much more severe deformations and mostly obtained submicrocrystalline or ultrafine grained CP-Ti structures, i.e.: with grain sizes above 100 nm (Woo-Jin Kim et al., 2006; Stolyarov et al., 2001a; Valiev et al., 2004; Salishchev et al., 2006; Valiev, 2005). Moreover, a direct comparison between the ductility characteristics is impossible since the tested samples often differ from one another by their dimensions and geometry. Fig. 6 shows that the elongation to failure obtained by hydrostatic extrusion fits well the tendency of the elongation to decrease with decreasing grain size diameter. The bigger grain size region up to ~ 120 nm was produced by a single operation of TE, ECAP, forging and their combination with CR, while smaller grain sizes < 120 nm were obtained by HPT, HE and a combination of forging with CR and ECAP with CE and TMT. Of these processes, HE is the only single process which yields nanosize grains in a massive (bulk) form.

3.2.3. Yield stress times elongation factor

The nanostructure obtained in a HE process is more homogeneous compared to those reported in literature. Hence, the appropriate grain size distribution effect that can induce additional ductility is strongly limited (Koch, 2003). The proposed multiplication factor which relates the strength and ductility $YS \times \epsilon_f$ (Krasilnikov et al., 2005), evaluated for GP-Ti processed by hydrostatic extrusion, seems to be comparable (9340 for $\varphi=5.5$) with literature data reported for other SPD processes. Fig. 7 shows the range of $YS \times \epsilon_f$ factors as a func-

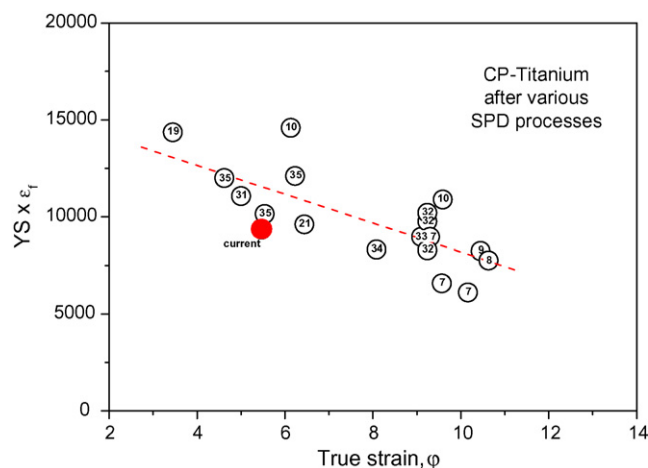


Fig. 7 – Multiplication factor of the yield stress times elongation to failure ($YS \times \epsilon_f$) vs. accumulated true strain for CP-Ti processed by various SPD processes; note: references in the circles.

tion of the accumulated true strain taken from literature and compared to our results. As compared to the HE results the data obtained with other SPD methods concern more complex and of much higher cumulated strain paths, such as for example ECAP + cold rolling (6120 for $\varphi = 10.2$) (Stolyarov et al., 2003), ECAP + cold extrusion (7760 for $\varphi = 10.6$) (Stolyarov et al., 2001a), ECAP + cold rolling + annealing (8240 for $\varphi = 10.5$) (Valiev et al., 2004) or uniform forging (10,890 for $\varphi \sim 8$) (Salishchev et al., 2006). None of literature data exceeds the yield stress (1245 MPa) obtained in present study and only some exceed (by 1–2%) the current strain to failure. Therefore, it is the ductility which needs further optimization after HE without damaging the strength which is already very high.

It can be concluded from Fig. 7 that the higher $YS \times \varepsilon_f$ factors are obtained for smaller accumulated true strains induced in single (non-combined) processes such as TE, ECAP, HPT, forging or HE and a combination of ECAP with TMT, while the lower values are reserved for large true strains associated with either single ECAP or its combination with CR and CE. This supports the observation that, for an advantageous combination of the strength and ductility to be achieved the deformation geometry and schedule are more important than the total value of accumulated true strain.

3.2.4. Microhardness

Microhardness is an important property, especially when the metal is in sliding contact with itself or other metals. The mean microhardness $HV_{0.2}$ developed during the HE steps is shown in Fig. 8. Each microhardness value is an average between 12 and 32 measurements. The value of $HV_{0.2}$ increased from the starting 2130 to 2745 MPa in the final wire subjected to 20 HE passes. Although, the total increase by almost 30% is not so spectacular as in the case of the tensile properties, it is superior to that in the initial coarse-grained CP-Ti. The microhardness increased with increasing reduction in the cross-section area (true strain), but this increase was not equally linear within the entire strain range. Four (or at least three) stages could be distinguished, Fig. 8; the

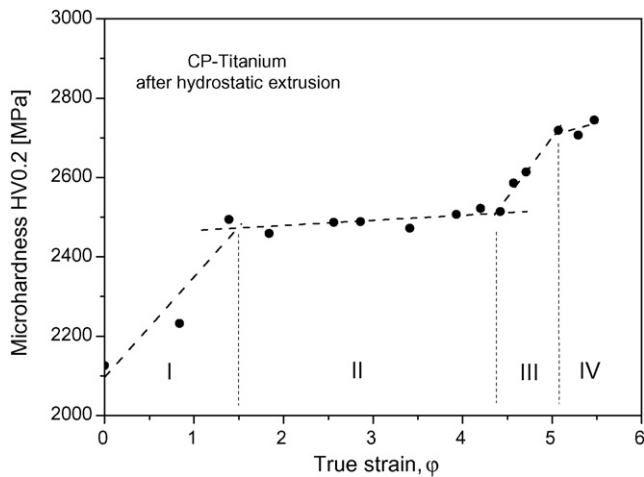


Fig. 8 – Strain hardening stages in CP-Ti during hydrostatic extrusion at room temperature.

first up to $\varphi \sim 1.5$ with the sharp increase of hardness from 2100 to 2500 MPa, the second between $1.5 < \varphi < \sim 4.4$ is a plateau ~ 2500 MPa, the third between $4.4 < \varphi < 5$ again with a sharp increase up to ~ 2720 MPa, and the final, fourth, above $\varphi > 5$ which resembles the saturated plateau. This shows, that the material strengthening proceeds differently at each stage of deformation. As commonly reported in literature, the deformation of titanium can be quite complex (Salem et al., 2002, 2005, 2006; Zeipper et al., 2005). This is connected with insufficient number of independent slip systems which can accommodate an arbitrary plastic strain in a polycrystalline material. Thus, the other processes, mainly widely reported deformation twinning are activated and observed to proceed in deformed CP-Ti (Salem et al., 2002, 2005, 2006). The competitive acting of the deformation twinning and dislocation slip systems is the reason of the complex strain hardening effects and of the occurrence of the distinct stages in the titanium strain-hardening response during deformation at room temperature.

3.2.5. True strain dependence of microhardness

The hardness-strain characteristic shown in Fig. 8, confirms the behaviour described above. The high strain-hardening rate in the first stage can be attributed to a coexistence of slip and twinning. Twinning divides the grains reduces the effective slip distances. There is a snowballing increase of the number of defects, which due to the limited slip planes in CP-Ti, interact and hinder their movement. Defects are getting trapped, introduce high internal stresses and, in consequence, cause a sharp increase of hardness. In the second stage, the accumulated stresses are released and the twin fraction saturates. The defects become partially annihilated and more ordered. Some flow localization due to adiabatic heating can also occur. The defects become mobile again, their density increases slowly and so does the hardness. The third stage is a consequence of similar processes to those proceeding in the first stage, with the difference in that the number of defects is drastically higher. The grains undergo severe refinement, the effective slip distance is reduced and an increase of

strain hardening via Hall-Petch (H-P) hardening occurs. Thus, the hardness characteristic slope rises again. Further mechanisms occurring within the nanosize grain range are difficult to describe, since they are probably the resultant of competing twinning and dislocation slip, each contributing to the final stress-strain response. The dynamic-recovery processes compete with strain-hardening ones, and their domination fluctuates with the progress in strain. Probably due to a continuous repetition of the saturation effects the resultant hardness does not change much. As concluded in Ref. Salem et al. (2006) the stress-strain response results in two competing effects of deformation twinning: hardening due to the shorter slip length and an increase in the hardness of the twinned regions, and softening due to the lattice reorientation of the twinned regions. Adiabatic heating whose effectiveness increases with diameter reduction also gives its important contribution at this strain range.

3.2.6. Microhardness uniformity

Fig. 9 shows the values of the coefficient of variation of the Vickers microhardness after hydrostatic extrusion of CP-Ti as a function of true strain. It can be seen, that the CV value decreases from ~ 0.04 after the initial extrusion stages to ~ 0.025 after the final stages, which suggests evident progress in the hardness distribution homogeneity as the HE develops (Kurzydowski and Ralph, 1995). The homogeneity is improved by the cumulative extrusion but also, at the final deformation stages (thinner wire gauges), the competition between strain hardening and adiabatic heating becomes stronger.

3.2.7. Transverse distribution of microhardness

A better visualization of microhardness profile smoothing (of uniformity improvement) gives the hardness profiles in the transverse direction after hydrostatic extrusion of CP-Ti rods and wires, Fig. 10. It can be seen, that the repeated passes of HE cause smoothing of the Vickers microhardness profiles. This results from the three main factors present during HE: the low reduction ratios during cumulative deformation,

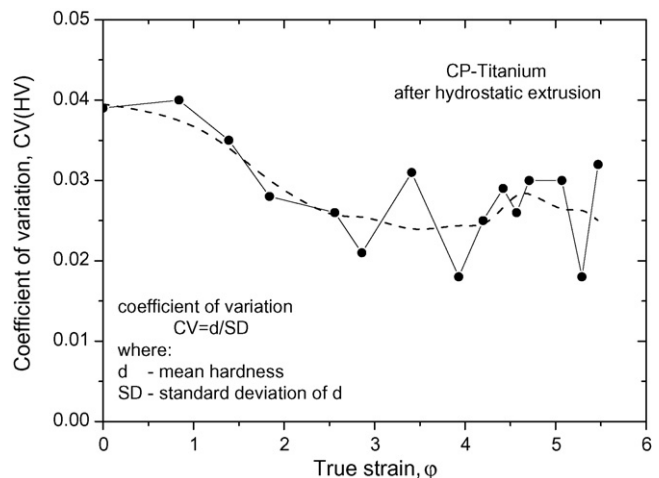


Fig. 9 – Values of the coefficient of variation for the Vickers microhardness after hydrostatic extrusion of CP-Ti as a function of true strain.

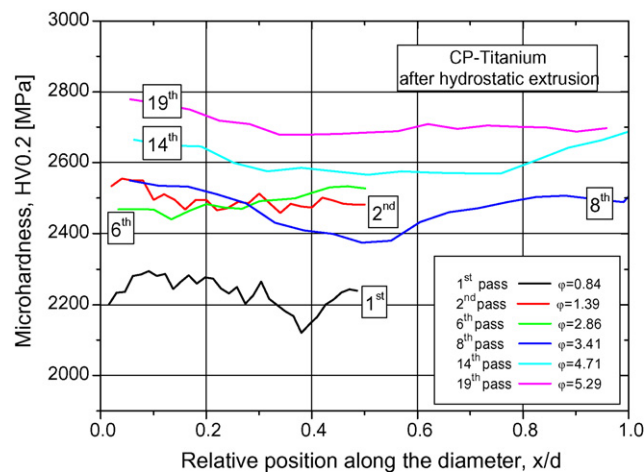


Fig. 10 – Vickers microhardness profile in the transverse direction after hydrostatic extrusion of CP-Ti.

good lubrication conditions and low semi-cone angles of the extrusion dies. This causes homogeneous deformation which does not introduce high distortion to the deformation grids. However, there is the another factor, namely the high strain rate, which acts negatively on the transverse hardness uniformity. The strain rates during extrusion of CP-Ti reached $3.28 \times 10^2 \text{ s}^{-1}$, which is a value two orders of magnitude higher than that in a standard ECAP process (Valiev and Langdon, 2006; Valiev et al., 2000) and may cause significant adiabatic heating during HE. This effect can be evaluated from the plastic work of deformation done during HE and, for CP-Ti, was estimated at $\sim 0.45T_m$, where T_m is the melting temperature of the worked material (1670°C for Ti). As one can see, it is a strong effect, which may result in thermally activated structural transformations occurring within the material (Pachla and Styczynski, 1984). This can be the factor responsible for the non-uniform distribution of the microhardness in the transverse direction of the extruded wires, Fig. 10. This is specially observed in the last passes characterized by the highest strain rates and the highest wire surface-to-volume ratios, where the temperature reaches a maximum. One of contributory factors to minimize the adiabatic heating is to minimize the extrusion pressure, i.e.: to minimize the applied strain per pass. In the current work the maximal true strain per pass does not exceed 0.84, but it seems to be still insufficiently small.

3.2.8. Comparison with other SPD processes

Comparison of the strength and ductility of CP-Ti deformed by hydrostatic extrusion and by other SPD techniques is presented in Table 2 and its visualization in Fig. 11. The other results were already compared and shown in Figs. 4, 6 and 7. Table 2 and Fig. 11 show, that very high yield strength (1245 MPa) and ultimate strength (1320 MPa) with moderate ductility (elongation to failure 7.5%) can be obtained in bulk, nanocrystalline CP-Ti deformed by a single process of cold hydrostatic extrusion. Thus far, the values close to those reported in the present work, were obtained by either ECAP or uniform forging processes followed by cold rolling, cold extrusion and additional annealing, i.e.: by complex treatments

Table 2 – Comparison between mechanical properties^a of CP-Ti processed by hydrostatic extrusion and by other severe plastic deformation (SPD) techniques

Processing state	Accumulated true strain	Mean grain diameter (nm)	Vickers microhardness HV (MPa)	Ultimate tensile strength UTS (MPa)	Yield stress YS (MPa)	Elongation to fracture ε_f (%)	Reference
Initial before HE	–	33,000	2,010	546	439	23.5	Current
After HE in 19 passes	5.47	47	2,745	1,320	1,245	7.5	Current
ECAP + cold extrusion (75%) + annealing	10.63	120	3,230	1,050	970	8	Stolyarov et al. (2001a)
ECAP	9.24	200	–	1,050	1,020	10	Vinogradov et al. (2001)
ECAP + cold rolling (55%)	10.16	150	3,000	1,050	1,020	6	Stolyarov et al. (2003)
HPT	7	80	2,800	1,380	1,050	–	Popov et al. (1997)
ECAP + TMT (80%)	6.23	70	–	1,150	1,100	11	Latysh et al. (2006)
Uniform forging + cold rolling (95%)	9.59	100	–	1,265	1,210	9	Salishchev et al. (2006)
Ti–Al–V solution treated alloy ^b	–	–	3,880	1,170	1,100	10	ASTM Grade 5

^a Sorted by yield stress.

^b Commercial alloy.

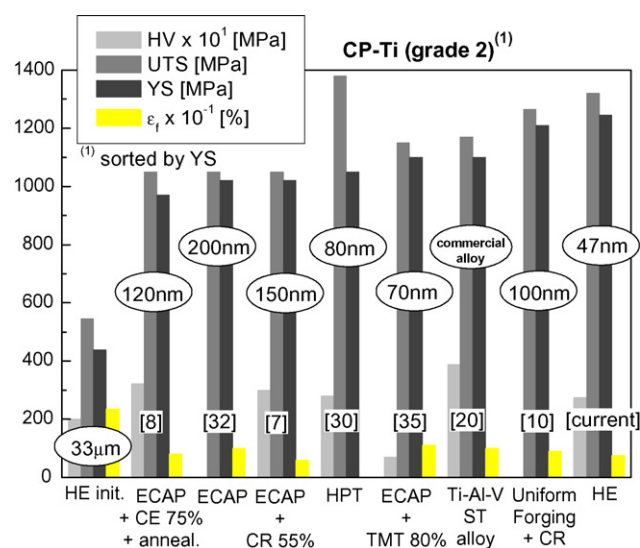


Fig. 11 – Comparison between mechanical properties of CP-Ti processed by hydrostatic extrusion and by other severe plastic deformation (SPD) techniques: note: commercial Ti-Al-V ST alloy given as the reference.

(Stolyarov et al., 2001a, 2003; Valiev et al., 2004; Salishchev et al., 2006). The strength obtained after hydrostatic extrusion is also higher than that of the Ti-6Al-4V solution treated (hardened) alloy (ASTM Grade 5), which makes it possible to replace a series of medical implants made of Ti-6Al-4V alloy by CP-Ti. It gives a great advantage since CP-Ti is chemically inert (in comparison to the toxic elements of Al and V) and biologically more compatible than Ti-6Al-4V alloy. This record-high strength was obtained in hydrostatically extruded CP-Ti due to the enormous grain refinement up to the nanometric scale generated in this material (mean equivalent grain diameter of 47 nm), Fig. 2. All the others SPD processes gave from 1.5 to 4 times as big grain sizes, so that their majority fell down to the UFG range. This was caused by the two reasons: they require the work piece to have relatively high ductility so that the processing must be conducted at elevated temperatures, or the complex processing is finalized by post-deformation annealing (final heat treatment).

This comparison presented in Fig. 11 shows that the most high-strength state of titanium is induced by hydrostatic extrusion and, in the second place by HPT for which a grain refinement of 80 nm was reported (Popov et al., 1997). This explains the substantial enhancement of strength after HE achieved in the present work, where the refinement below 50 nm was obtained. It should also be noted, that HE involves not only a simple (pure) shear mechanism which is the case in HPT, but also additional dislocation slip systems. Higher strength after HE occurs for lower accumulated strains compared to those in simple shear processes as HPT (Popov et al., 1997; Sergueeva et al., 2001; Stolyarov et al., 1999), ECAP (Vinogradov et al., 2001; Stolyarov et al., 2001b; Latysh et al., 2006) or TE (Stolyarov et al., 2005). The second important matter is, that nanostructured CP-Ti produced by HE has comparable ductility to the commercial Ti-6Al-4V alloy, which is widely used in medicine, Table 2. In compari-

son to other deformation techniques severe HE deteriorates the ductility only slightly, Fig. 6, in extent corresponding to differences in strength. It is not significant decrease, by 1.5–3.5%, as compared to strongest nanostructures obtained by others, Table 2. It can be due to much higher homogenization, more healed nanostructure and much lower grain size obtained after HE. Thus, the ductility does not deteriorate significantly during tension since more grain boundaries causes easier deformation accommodation by slip and rotation. This holds out good prospects for future commercial applications.

The problem for commercialization can create the modulus of elasticity which for CP-Ti and Ti-alloys is much higher (105–120 GPa) than that of the human being bone (maximum 30 GPa). It can results in bone resorption (Gordin et al., 2004). Modulus of elasticity is the vector quantity which strongly depends on texture. The wire after HE is always characterized by the specific texture. Decrease of the modulus of elasticity after HE can be expected if the suitable material texture is generated during the material deformation. However, it was not a matter of investigation in present work.

3.2.9. Hall-Petch relation

The enhancement of the yield stress and hardness in the materials processed by various SPD processes is shown in Fig. 12. This is the most frequently used relationship which relates the mechanical properties with the microstructure parameters (mean grain diameter), i.e.: the Hall-Petch relation. The strength and hardness dependences on the mean grain size in CP-Ti reported in literature and in the present work are compared in Fig. 12(a and b), respectively, in the range below 1 μ m down to 50 nm (our result). However, a higher refinement for CP-Ti, even down to \sim 10 nm, were reported in Sergueeva et al. (2001), but the authors did not describe clearly the methods of sample preparation. According to the authors best knowledge, the minimum grain sizes in CP-Ti (between 80 and 120 nm) were obtained with the HPT technique (Popov et al., 1997; Sergueeva et al., 2001) and \sim 120 nm in the transverse fibrous grains produced by a combination of ECAP and extrusion (Stolyarov et al., 2001a). It follows from the above that only ECAP and extrusion offers perspectives of producing applicable bulk titanium performs. One can see in Fig. 12, that the H-P relationships are not congruent depending on whether the strength or hardness is taken into consideration. For the YS dependence the linear fit is more suitable, Fig. 12(a), while the hardness dependence reveals the slope change from positive (material hardening with decreasing grain size) to negative (material softening), Fig. 12(b). The threshold between these two behaviours falls at \sim 120 nm, i.e. somewhere around the point which is commonly considered to be the UFG/NC structural border. The H-P hardness dependence is cited more frequently in literature, what is obvious from the fact, that many UFG and NC materials obtained do not allow of proper specimens for tensile tests to be prepared.

According to the current analysis of the CP-Ti results between 50 nm and 1 μ m, the H-P hardness dependence, Fig. 12(b), can be described by the following relationship:

$$HV = 2034 + 12088d^{-1/2}(\text{MPa}) \quad (\text{for grains} > 120 \text{ nm}) \quad (1)$$

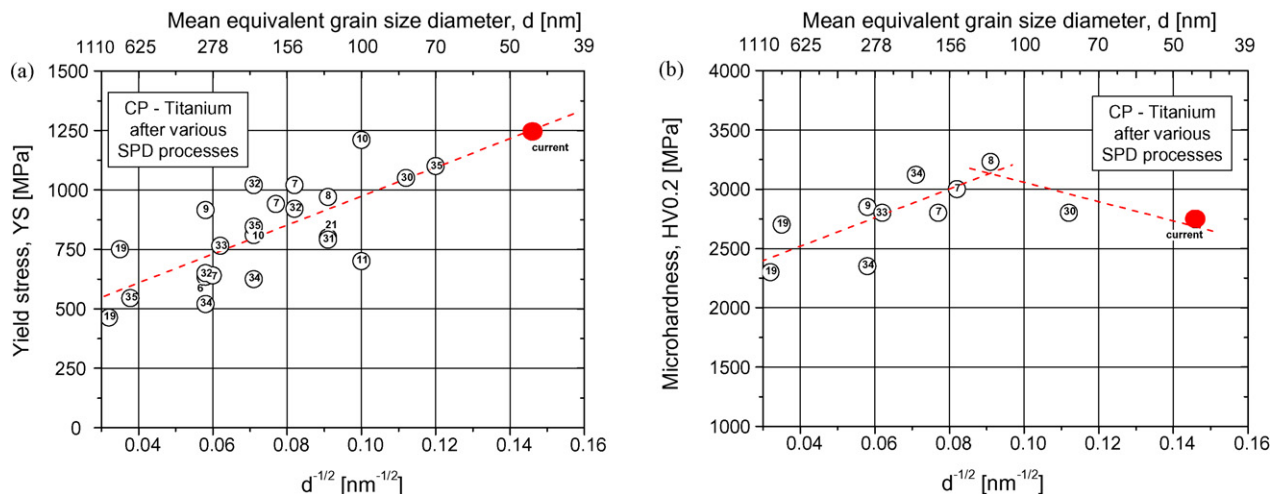


Fig. 12 – The Hall-Petch relations of (a) yield stress, and (b) Vickers microhardness, for CP-Ti processed by various SPD processes; note: references in the circles.

and

$$HV = 3870 - 8130d^{-1/2}(\text{MPa}) \quad (\text{for grains} < 120 \text{ nm}) \quad (2)$$

Eq. (1) is in 5% agreement when the current data are completed with the results for the ultra-nano CP-Ti grains down to 10 nm, given in Ref. [Sergueeva et al. \(2001\)](#). However, for 10 nm grains in CP-Ti the Eq. (2) predicts microhardness of ~ 1300 MPa (Eq. (2)), while Ref. [Sergueeva et al. \(2001\)](#) shifts it to an extremely high value of ~ 5560 MPa. It is an unreasonably high value, which cannot be explained even when departing from the known empirical equation of $HV = 3 YS$ ([Popov et al., 1997](#)). To determine more accurately the CP-Ti H-P hardness dependence in the ultra-nano grain region further experiments are required. The main problem is to fabricate appropriate materials with grains within this size range.

An analysis of the H-P yield stress dependence, Fig. 12(a), of CP-Ti between 50 nm and 1 μm has led to the equation:

$$YS = 366.5 + 6067d^{-1/2}(\text{MPa}) \quad (3)$$

However, a more careful analysis of these results shows that at an approximately 120 nm grain size, the change in the H-P slope may also occur in the YS dependence. It is the same threshold point which appears in the H-P hardness dependence. The scatter of data does not allow formulating relationships, although this will be possible when more experimental data are available. A calculation by linear fit gives $YS \sim 2300$ MPa for 10 nm grains, which is higher by 1000 MPa than the maximum value in the present study, thus far Table 2. The authors believe that such a value is not attainable in CP-Ti without losing the material integrity and that the flattening on the H-P yield stress dependence for smaller grain sizes (below 100 nm) must occur.

Considering future applications of CP-Ti either in biomedicine or transportation one should notice, that the strength values obtained after hydrostatic extrusion are comparable with those of the best tool steels available in the market, for example AISI H13 steel (Uddeholm Orvar)

with $YS = 1280$ MPa. Therefore, the properties of CP-Ti after HE make this material equally suitable for structural applications.

4. Conclusions

The effect of severe plastic deformation by hydrostatic extrusion on the structure and mechanical properties of CP-Ti wire was studied.

- HE with total accumulated true strain of 5.5 causes a high strength ($UTS > 1300$ MPa and $YS \sim 1250$ MPa, the highest ever reported for bulk samples). These values are higher than that in the solution treated Ti-6Al-4V commercial alloy. Ductility is still retained at the level characteristic of the other bulk SPD treated materials ($\sim 7.5\%$).
- Repeated cycles of hydrostatic extrusion causes considerable changes in the Ti microstructure resulting in a large refinement of the microstructure down to the nanometre size. The equiaxed grains of ~ 50 nm in a transverse section and elongated grains located in the lamellar microstructure in a longitudinal section are observed. Both sections show grains with high-angle grain boundaries and a high dislocation density, the smallest ever reported for bulk samples.
- Good combination of the strength and ductility depends on the deformation geometry and schedule more than on the accumulated true strain. Therefore, the authors believe that controlled post-deformation annealing of the structures after HE will yield more enhancement of ductility, which needs to be further optimized.
- The present results revealed the possibility of fabricating long-length high strength nanocrystalline CP-Ti semi-products using the hydrostatic extrusion process. This technology enables enhancing the strength almost by a factor of 3 compared to the initial state and by more than 10% compared to that of the commercial Ti-6Al-4V alloy which contains potentially toxic elements. Thus, semi-products made of CP-Ti can be used for medical applications which require high strength and biocompatibility (e.g. dental implants).

Acknowledgements

This work was supported by the Polish Ministry of Science and Informatics grant No: 4 T08A 04525. Assistance by Dr. Z. Witczak from IHPP PAS in mechanical tests is gratefully acknowledged.

REFERENCES

- <http://www.matweb.com> Alpha/Beta Titanium Alloys (Ti-6-4; UNS R56400; ASTM Grade 5 titanium; UNS R56401 (ELI); Ti6Al4V).
- Dinda, G.P., Rösner, H., Wilde, G., 2005. Synthesis of bulk nanostructured Ni, Ti and Zr by repeated cold-rolling. *Scripta Mater.* 52, 577–582.
- Garbacz, H., Lewandowska, M., Pachla, W., Kurzydłowski, K.J., 2006. Structural and mechanical properties of nanocrystalline titanium and 316LVM steel processed by hydrostatic extrusion. *J. Microsc.* 223 (3), 272.
- Gordin, D.M., Gloriant, T., Texier, G., Thibon, I., Ansel, D., Duval, J.L., Nagel, M.D., 2004. Development of a β -type Ti-12Mo-5Ta alloy for biomedical applications: cytocompatibility and metallurgical aspects. *J. Mater. Sci.: Mater. Med.* 15, 885–891.
- Koch, C.C., 2003. Optimization of strength and ductility in nanocrystalline and ultrafine grained metals. *Scripta Mater.* 49, 657–662.
- Krasilnikov, N., Lojkowski, W., Pakiel, Z., Valiev, R., 2005. Tensile strength and ductility of ultra-fine-grained nickel processed by severe plastic deformation. *Mater. Sci. Eng. A* 397, 330–337.
- Kurzydłowski, K.J., 2006a. Physical, chemical and mechanical properties of nanostructured materials. *Mater. Sci.* 42 (1), 85–94.
- Kurzydłowski, K.J., 2006b. Hydrostatic extrusion as a method of grain refinement in metallic materials. *Mater. Sci. Forum* 503–504, 341–348.
- Kurzydłowski, K.J., Ralph, B., 1995. *The Quantitative Description of the Microstructure of Materials*. CRC Press.
- Latysh, V., Kralics, Gy., Alexandrov, I., Fodor, A., 2006. Application of bulk nanostructured materials in medicine. *Curr. Appl. Phys.* 6, 262–266.
- Nagasekhar, A.V., Chakkingal, U., Venugopal, P., 2006. Candidature of equal channel angular pressing for processing of tubular commercial purity-titanium. *J. Mater. Process. Technol.* 173, 53–60.
- Pachla, W., Styczyński, L., 1984. Structure and strength of polycrystalline copper during hydrostatic extrusion with reduction up to $R=100$. *Metal Sci.* 18, 22–26.
- Pachla, W., Kulczyk, M., Swiderska-Sroda, A., Lewandowska, M., Garbacz, H., Mazur, A., Kurzydłowski, K.J., 2006. In: Juster, N., Rosochowski, A. (Eds.), *Nanostructuring of Metals by Hydrostatic Extrusion, ESAFORM 2006*. Glasgow, United Kingdom, pp. 535–538.
- Popov, A.A., Pyshmintsev, I.Yu., Demakov, S.L., Illarionov, A.G., Lowe, T.C., Sergeyeva, A.V., Valiev, R.Z., 1997. Structural and mechanical properties of nanocrystalline titanium processed by severe plastic deformation. *Scripta Mater.* 37 (7), 1089–1094.
- Saito, Y., Utsonomiya, H., Tsuji, N., Sakai, T., 1999. Novel ultra-high straining process for bulk materials—development of the accumulative roll-bonding (ARB) process. *Acta Mater.* 47 (2), 579–583.
- Salem, A.A., Kalidindi, S.R., Doherty, R.D., 2002. Strain hardening regimes and microstructure evolution during large strain compression of high purity titanium. *Scripta Mater.* 46, 419–423.
- Salem, A.A., Kalidindi, S.R., Semiati, S.L., 2005. Strain hardening due to deformation twinning in α -titanium: constitutive relations and crystal-plasticity modelling. *Acta Mater.* 53, 3495–3502.
- Salem, A.A., Kalidindi, S.R., Doherty, R.D., Semiati, S.L., 2006. Strain hardening due to deformation twinning in α -titanium: mechanisms. *Metal. Mater. Trans. A* 37A, 259.
- Salishchev, G.A., Galeev, R.M., Malysheva, S.P., Myshlyayev, M.M., 1999. Structure and density of submicrocrystalline titanium produced by severe plastic deformation. *NanoStruct. Mater.* 11 (3), 407–414.
- Salishchev, G.A., Galeev, R.M., Malysheva, S.P., Zherebtsov, S.V., Mironov, S.Yu., Valiakhmetov, O.R., Ivanisenko, E.I., 2006. Formation of submicrocrystalline structure in titanium and titanium alloys and their mechanical properties. *Metal Sci. Heat Treat.* 48 (1/2), 63–69.
- Segal, V.M., 2002. Severe plastic deformation: simple shear versus pure shear. *Mater. Sci. Eng.* A338, 331–344.
- Sergueeva, A.V., Stolyarov, V.V., Valiev, R.Z., Mukherjee, A.K., 2001. Advanced mechanical properties of pure titanium with ultrafine grained structure. *Scripta Mater.* 45, 747–752.
- Stolyarov, V.V., Zhu, Y.T., Lowe, T.C., Islamgaliev, R.K., Valiev, R.Z., 1999. A two step SPD processing of ultrafine-grained titanium. *NanoStruct. Mater.* 11 (7), 947–954.
- Stolyarov, V.V., Zhu, Y.T., Lowe, T.C., Valiev, R.Z., 2001a. Microstructure and properties of pure Ti processed by ECAP and cold extrusion. *Mater. Sci. Eng.* A303, 82–89.
- Stolyarov, V.V., Zhu, Y.T., Alexandrov, I.V., et al., 2001b. Influence of ECAP routes on the microstructure and properties of pure Ti. *Mater. Sci. Eng. A* 299 (1/2), 59–67.
- Stolyarov, V.V., Zhu, Y.T., Alexandrov, I.V., Lowe, T.C., Valiev, R.Z., 2003. Grain refinement and properties of pure Ti processed by warm ECAP and cold rolling. *Mater. Sci. Eng.* A343, 43–50.
- Stolyarov, V.V., Beigel'zimer, Ya.E., Orlov, D.V., Valiev, R.Z., 2005. Refinement of microstructure and mechanical properties of titanium processed by twist extrusion and subsequent rolling. *Phys. Metals Metall.* 99 (2), 204–211.
- Valiev, R., 2004. Nanostructuring of metals by severe plastic deformation for advanced properties. *Nat. Mater.* 3, 511–516.
- Valiev, R.Z., 2005. Recent progress in developing bulk nanostructured SPD materials with unique properties. *Solid State Phenom.* 101–102, 3–12.
- Valiev, R.Z., Langdon, T.G., 2006. Principles of equal-channel angular pressing as a processing tool for grain refinement. *Prog. Mater. Sci.* 51, 881–981.
- Valiev, R.Z., Islamgaliev, R.K., Alexandrov, I.V., 2000. Bulk nanostructured materials from severe plastic deformation. *Prog. Mater. Sci.* 45, 103–189.
- Valiev, R.Z., Alexandrov, I.V., Zhu, Y.T., Lowe, T.C., 2002. Paradox of strength and ductility in metals processed by severe plastic deformation. *J. Mater. Res.* 17 (1), 5–8.
- Valiev, R.Z., Stolyarov, V.V., Rack, H.J., Lowe, T.C., 2004. SPD-processed ultra-fine grained Ti materials for medical applications. In: Shrivastava, S. (Ed.), *Materials and Processes for Medical Devices I*. ASM International, Materials Park, OH, pp. 362–367.
- Vinogradov, A.Y., Stolyarov, V.V., Hashimoto, S., Valiev, R.Z., 2001. Cyclic behavior of ultrafine-grain titanium produced by severe plastic deformation. *Mater. Sci. Eng. A* 318, 163–173.
- Woo-Jin, K., Chang-Young, H., Ho-Kyung, K., 2006. Fatigue strength of ultra fine grained pure Ti after severe plastic deformation. *Scripta Mater.* 54, 1745–1750.
- Zeipper, L.F., Zehetbauer, M.J., Holzleithner, Ch., 2005. Defect based micromechanical modelling and simulation of nanoSPD CP-Ti in post-deformation. *Mater. Sci. Eng. A* 410–411, 217–221.